Heliyon 8 (2022) e10775

Contents lists available at ScienceDirect

Heliyon

journal homepage: www.cell.com/heliyon

Research article

Efficacy of bivalent *CEACAM6/4*-1BBL genetic vaccine combined with anti-PD1 antibody in MC38 tumor model of mice

Yuzhen Li [1], Xiaodan Zhu [1], Jianliang You, Baonan Zhang, Xiaona Huang, Chunhui Jin [*]

Department of Oncology, Wuxi Hospital Affiliated to Nanjing University of Chinese Medicine, Wuxi, China

ARTICLE INFO

Keywords:
Colorectal cancer
Anti-tumor immunotherapy
Genetic vaccine
CEACAM6
4-1BBL
Anti-PD1 drug

ABSTRACT

We used mouse CRC cell line (MC38) to establish a heterotopic mouse model, and applied [^{89}Zr]-labeled PD-L1 antibody KN035 for PET imaging. Attenuated *Salmonella typhimurium* 3261 was used as an anti-tumor vaccine, and the combined anti-tumor immunotherapy with bivalent genetic vaccine and anti-PD1 antibody Nivolumab was conducted. MicroPET was performed to observe the changes of tumor tissues and expression of PD-L1. We found that the recombinant double-gene plasmids were stably expressed in COS7 cells. Study results showed the combined immunotherapy improved the effectiveness over genetic vaccine alone. This study supports that combination of genetic vaccines and anti-immunocheckpoint immunotherapy can inhibit MC38 tumor growth.

1. Introduction

Colorectal cancer (CRC) is the second leading cause of cancer death worldwide, with poor 5-year overall survival after surgery [1, 2]. The 5-year survival rate for patients with distant metastases was about 12% [3]. At present, chemotherapy is the main treatment means for local metastasis of CRC, but the effect is not significant; for patients with distant metastasis, the efficiency of chemotherapy is even lower [4, 5]. Nowadays, immunoregulation and immunotherapy for cancer diseases has gained due attention. As tumor progression in consequence of resistance to chemical and radiotherapy remains sensitive and appropriate for immunotherapy [6, 7], immunotherapy should be a better choice for CRC patients. The most effective therapy now for activating anti-tumor immunity is to block the suppressive immunoregulatory proteins such as immunocheckpoint ligands and receptors. Tumor immunotherapy has become a hot spot since the emergence of inhibitors of programmed cell death protein-1 (PD1/CD279). Blocking the PD1/PD-L1 signal pathway with anti-PD1/PD-L1 monoclonal antibody has shown excellent anti-tumor efficacy in a variety of solid tumors. In CRC tumor microenvironment, PD1 is up-regulated in CD8+ T cells, resulting in the disturbance of cytokines and perforin production [8, 9]. The expression of PD-L1 in CRC cells in tumor microenvironment is inversely proportional to T cell density. PD1 expression was found in CD4+ and CD8+ T cells in peripheral blood of CRC patients after surgery, which was associated with the impaired T cell function [10]. These reports show that blocking the PD1/PD-L1 pathway is a feasible treatment strategy for CRC.

Genetic immunotherapy is one of the hotspots in cancer immunotherapy research. In cancer genetic immunotherapy, a gene fragment encoding a tumor protein is inserted into the multiple cloning sites in a eukaryotic expression plasmid, and the encoded exogenous proteins can be expressed in the host cells and bind to MHC class I and II molecules in the form of endogenous peptides, thus induce specific immunity, especially cellular immunity, to tumor cells expressing related proteins [11, 12]. However, due to the low expression of MHC class I molecules in tumor cells, the lack of co-stimulatory signals, and the lack of immune factors associated with synergistic anti-tumor effects through multiple signaling pathways, these genetic vaccines are unsuccessful to induce effective anti-tumor immune responses to kill tumor cells. At present, therapeutic methods with combined multiple synergistic immunoregulatory genes are being developed from initially single tumor gene for tumor immunotherapy. For example, tumor vaccines that combine tumor specific antigens with co-stimulatory molecules and cytokines which activate multiple signaling pathways can induce tumor specific immunity and enhance immune responses. The combined genetic vaccines are a new strategy for tumor immunotherapy [13, 14].

Carcinoembryonic antigen (CEA) is a promising tumor immunotherapy target, and CEA-derived vaccine has been used to activate B cells and T cell immunity [15, 16]. Carcinoembryonic antigen-related cell adhesion molecule 6 (CEACAM6), like CEA, belonging to the

* Corresponding author.
E-mail address: wxzy013@njucm.edu.cn (C. Jin).
[1] These authors equally contributed.

https://doi.org/10.1016/j.heliyon.2022.e10775
Received 6 March 2022; Received in revised form 13 July 2022; Accepted 20 September 2022

carcinoembryonic antigen gene family and immunoglobulin superfamily, is located in the q13.2 zone of the chromosome 19 and encodes CEACAM6 protein containing 344 amino acids on the cell membrane surface. Many experiments show that CEACAM6 plays important roles in tumor cell adhesion, inhibition of apoptosis, differentiation blockade, cell polarity loss, invasion and metastasis [17, 18, 19]. CEACAM6 is also involved in tissue structure and colon cell differentiation [20]. In researches of colorectal cancer, the expression of CEACAM6 has been found to be associated with tumor stages and lymph node metastasis, and the risk of postoperative recurrence can be classified according to the degree of its expression, thus CEACAM6 up-regulation is considered to be an independent predictor of poor survival in colorectal cancer patients [21]. Therefore, CEACAM6 is a better tumor marker than CEA and may be a more promising target for the therapy of solid tumors.

4-1BB, also known as CD137, a type I glycoprotein and a member of tumor necrosis factor receptor superfamily, was first identified in research using ConA to activate helper and cytotoxic T cell receptors [22]. 4-1BB is a co-stimulatory receptor to activate T cells after tumor cell antigen recognition. 4-1BB/4-1BBL are a pair of important co-stimulatory molecules, which can enhance immune responses to various antigens, and co-stimulate the production of T cell-related cytokines and the proliferation, maturation and survival of T cells [23, 24, 25]. Studies have shown that 4-1BB is expressed in many immune cells besides T cells and its natural ligand 4-1BBL and agonists such as agonist-like antibody can induce strong anti-tumor responses of many cell types, and thus it has been widely used in the development of anti-tumor immunotherapy [26]. The expression level of 4-1BB was directly correlated with CRC staging and degree of infiltration [27]. The expression of 4-1BBL is low in colon cancer tissue, which leads to weakened interaction between T cells, macrophages and tumor cells, thus causing immune escape. 4-1BB agonist is effective in the treatment of CRC with liver metastasis. Previous studies have shown that recombinant attenuated Salmonella typhimurium containing the 4-1BBL gene induces high levels of 4-1BBL expression in dendritic cell and other immune cells [28]. Vaccination with the 4-1BBL gene vaccine has been shown to inhibit the development of CRC in rats via enhancing T cell immunity [29]. However, the efficacy of genetic vaccine including *CEACAM6/4*-1BBL genes combined with immunocheckpoint inhibitor on CRC has not been reported.

Recombinant attenuated intracellular bacteria, such as *Salmonella* and *Shigella*, can deliver nucleic acid vaccines via spontaneous mucosal infections [30]. Attenuated *Salmonella typhi* enters tumor cells through type III secretion system, and the bacterial-derived antigens after lysis can be expressed on the surface of tumor cells to arouse anti-tumor immune effect [31]. Attenuated *Salmonella typhimurium*, as a good delivery vehicle for gene vaccines, has become a development concern for gastrointestinal cancer vaccine therapy [32, 33]. In our previous studies, we introduced the constructed eukaryotic expression plasmid containing *CEACAM6* and *4*-1BBL genes into attenuated *Salmonella typhimurium* 3261 (SL3261) and obtained a stable transformation strain, and used it for the treatment of dimethylhydrazine (DMH)-induced intestinal tumor in rats and achieved significant therapeutic effect [34, 35]. It was found that the bivalent vaccine could increase the infiltration of CD3+ T cells, CD8+ T cells and NK cells, enhance T cell activity, decrease the infiltration of regulatory T cells, promote Th1 polarization, and inhibit Th2 and Th17 polarization, stimulating specific and non-specific anti-tumor immune responses. Therefore, we assume that enhancing anti-tumor immunity with bivalent genetic vaccine may promote the tumor have local immunogenicity and become immunologically "hot tumor", and combining it with PD1 inhibitor may improve the efficacy of anti-tumor immunotherapy.

In this study, mouse colon cancer MC38 cells were used to establish a heterotopic tumor mouse model, and [^{89}Zr]-labeled PD-L1 antibody was used for imaging. The eukaryotic expression plasmid containing *CEACAM6/4*-1BBL genes was introduced into the SL3261 to obtain stable transformation strain, and then anti-tumor immunotherapy and observation were carried out with combination of the genetic bivalent vaccine and anti-PD1 antibody. At the same time, microPET was performed to monitor the changes of tumor tissues and the expression of PD-L1, so as to non-invasively and dynamically observe and evaluate tumor and therapeutic effect of the combined immunotherapy.

2. Materials and methods

2.1. Construction and identification of double-gene plasmids

The plasmids were purchased from Clontech Laboratories, Inc. (Mountainview, CA, USA). Construction, amplification and extraction of pIRES-CEACAM6-4-1BBL double gene plasmid were reported in our earlier reports [34, 35]. The selection of splicing enzymes and the identification of plasmid are very important since this is a double-gene combined vaccine. Enzyme contamination should be avoided in transformation, and the transformation and detection conditions should be optimized by housekeeping gene as positive control. The transformed bacteria E. Coli should be coated to a flat plate to disperse into single bacterium colonies, and cultured under suitable conditions. When a single bacterium grows into a colony, finally select the cloned bacteria for extraction and identification.

2.2. Transfection of genetically modified plasmids

Method for eukaryotic expression system transfection is as previously published methods [34, 35]. COS7 cell line was purchased from American Type Culture Collection Center (Manassas, VA, USA; ATCC Number: CRL-1651). The COS7 cells were transfected with liposome. COS7 cells were cultured in DMEM medium containing 10% fetal bovine serum (FBS) (Gibco, Grand Island, NY), taken in logarithmic growth phase, digested with trypsin, and inoculated into 6-well culture plate in a 5% CO_2 incubator at 37 °C for 24 h (the cell growth density was 80%–90%). The extracted plasmids were transfected into COS7 cells with Lipofectamine2000 liposomes (Invitrogen), and the control group was treated with the same amount of blank liposomes. The transfection procedure was in accordance with the instructions of Lipofectamine2000 Reagent kit.

2.3. Polymerase chain reaction (PCR)

Reverse transcript (RT)-PCR identification of objective genes was performed. The total RNA was extracted with Trizol reagent, purified and the concentration was adjusted, then the cDNA was generated by reverse transcription. Reaction system: total RNA 2 μL, RNase inhibitor 0.5 μL, oligo-dT18 2 μL, cooling on ice after 65 °C for 5 min; then 5× RT buffer 4 μL, 10 mM dNTPs 2 μL, RNase inhibitor 0.5 μL, M-MLV reverse transcriptase 1 μL, and double distilled water were added to total volume of 20 μL; after 1 h at 37 °C and 10 min at 70 °C, the system was cooled on ice. All the used primers were synthesized by Shanghai Bioengineering Co., Ltd. *CEACAM6* gene forward primer: 5-CAGAGCCAAACAACAGAT-3; reverse primer: 5-CATTATTACTTATGCTGACCT-3. *4*-1BBL gene forward primer: 5-GCTCTAGAGCCACCATGGACCAGCACGCACTTG-3; reverse primer: 5-GGCGGCCGCGTCATCCCTGAGGGGGGTC-3. PCR reaction system: 10× buffer 5 μL, Mg^{2+} solution 4 μL, dNTP 1 μL, forward primer 1 μL, reverse primer 1 μL, Tag enzyme 0.3 μL, template cDNA 3 μL. Reaction conditions: pre-denaturation at 95 °C for 10 min; 95 °C for 20 s, 52 °C for 30 s, 72 °C for 1 min, 35 cycles; more extension at 72 °C for 7 min, and 4 °C forever. Agarose gel electrophoresis was performed with PCR products 15 μL and DNA marker 5 μL, and the results were observed and analyzed by Gel imaging and analysis system (HUADIAN DH2000).

2.4. Protein expression and Western blot identification

After transfection with double-gene plasmids, COS7 cells were cultured at 37 °C for 4 h, and then changed to fresh DMEM containing

10% FBS. A plasmid-free negative control group was established. Cells were collected for test 48 h after transfection. The cells were mixed within ice-precooled protein lysates (l mM PMSF, pH7.4), broken up by ultrasonic cracker, centrifuged at 4 °C, 12000 rpm for 15 min, and the supernatant was taken for loading sample preparation and Western blotting assay. Antibodies used: anti-4-1BBL mouse monoclonal antibody (sc-398933, Santa cruz, 1:1000), anti-CEACAM6 rabbit monoclonal antibody (ab235139, Abcam, 1:1000), anti-PD-L1 rabbit polyclonal antibody (ab233482, Abcam, 1:1000), and anti-GAPDH mouse monoclonal antibody (ab125247, Abcam, 1:5000), and secondary antibodies (Beyotime Biotechnology). The follow-up WB method was as reported [36].

2.5. Transformation of attenuated SL3261 with recombinant plasmids

Attenuated SL3261 was primarily provided from the laboratory of Professor Stocker of Stanford University (Stanford, CA, USA) and then on conserved in our laboratory. SL3261 bacteria in 10% glycerol stored at −80 °C was inoculated into non-resistant LB plate and cultured at 37 °C for 18 h. The selected single colony was cultured in 2 mL LB at 37 °C for 12 h with oscillation, and inoculated in 50 mL LB in 1:100 dilution and oscillated until the OD600 was about 0.4. The bacterial culture was transferred into a 50 mL aseptic centrifuge tube in ice for 20 min, centrifuged at 4 °C at 3000 rpm for 10 min, and the supernatant was discarded. Add pre-cooled sterile deionized water to resuspend the bacteria, centrifuge at 4 °C at 3000 rpm for 10 min and discard the supernatant; repeat this procedure twice to wash the bacteria fully. Ice-cold 10% glycerol was used to suspend the bacteria, and centrifuge at 4 °C at 3000 rpm for 10 min and discard the supernatant. The bacteria were suspended in 2 mL pre-cooled 10% glycerol and packed in pre-cooled EP tube (150 μL) for use or store at -80 °C. Susceptible Salmonella SL3261 150 μL was added into pre-cooled 2 mm electro-conversion cup, 1 μL empty carrier plasmids or recombinant expression plasmids were added and fully mixed, resting in ice-bath for 30 min. The parameters of the electro-converter were as follows: voltage 2500 V, resistance 200 Ω, capacitance 25 F. Take out the electro-conversion cup and dry the water on the outside before electro-transformation. After electro-transformation, 500 μL LB preheated at 37 °C was added immediately. The bacteria-containing liquid was transferred into EP tube, and cultured in a shaker at 37 °C and 100 r/min for 1 h. Centrifuge the culture at 4000 rpm for 5 min, discard the supernatant, resuspend the bacteria, coat them into LB plate with ampicillin, and incubate overnight at 37 °C. Positive clones were picked out and the bacteria were amplified. Three clones were inoculated into 4 mL LB medium containing ampicillin, incubated at 37 °C and 180 rpm in a shaker overnight, and plasmids were extracted and identified by PCR.

2.6. Animals and MC38 tumor model

SPF-grade C57BL/6 female mice, aged 6–8 weeks, were obtained from Beijing Vital River Laboratory Animal Technology Co., Ltd., and kept in clean animal room of Jiangsu Institute of Parasitic Diseases. The temperature was maintained at 24 ± 2 °C, the relative humidity was 60% ± 5%, and the light/dark cycle was 12/12 h. The bedding, drinking water and food were all sterilized. The feeding, body hair and activity of the animals were observed, and the body weights of the mice were measured weekly. All experiments with animals of this study were approved by the Animal Care and Research Ethics Committee of the Wuxi Hospital affiliated to Nanjing University of Chinese Medicine. Culture and modeling injection of mouse colon cancer cell line MC38 cells was based on reference [37]. MC38 cells were cultured in RPMI-1640 medium (Invitrogen, Carlsbad, CA) supplemented with 10% FBS and 1% PS (100 U/mL penicillin and 100 μg/mL streptomycin) at 37 °C and 5% CO_2. MC38 cells were injected subcutaneously into the medial left forelimb of mice. Briefly, 1 × 10^6 cells of MC38 cells were injected for one mouse. The growth of MC38 heterotopic tumor was observed by microPET scans 1 week after model establishment. Xenograft tumor sizes of the model mice were measured every two days. Short and long tumor diameters, tumor volume, and body weight were measured. When the xenograft tumor grew to a volume of 150–200 mm^3, the mice were used for PET imaging study. Drugs were given at about two weeks after the model establishment.

2.7. Grouping and treatment

According to microPET scanning results, the CRC model mice were equally divided into three groups, the control group, the pIRES-CEACAM6-4-1BBL/SL3261 group, and the pIRES-CEACAM6-4-1BBL/SL3261 + anti-PD1 antibody group. The control group mice were given vehicle, and the other two groups were given the prepared bivalent vaccine of pIRES-CEACAM6-4-1BBL/SL3261 0.2 mL (10^9 stable transformants/mL) per mouse. All the mice were deprived of water for 2 h before vaccine administration via gavage. The anti-PD1 antibody Nivolumab solution (2 mg/mL) was administered by tail vein injection at a dose of 20 mg/kg. All mice were therapeutically administrated according to grouping two weeks after the modeling transplantation injection. Then the mice were scanned with microPET imaging, and after the last scanning, the mice were anesthetized with 2% pentobarbital sodium at 65 mg/kg intraperitoneally. After that, the mice were executed by dislocation of cervical vertebra and the tissues were harvested for analysis.

2.8. Immunohistochemical (IHC) assay

The tumor tissues (including the tumor and its surrounding normal tissue) were taken and immersed in 10% neutral formalin. After dehydration, diaphaneity, wax dipping and embedding, the specimens were sectioned to 5 μm slices. The IHC staining (with anti-PD-L1 rabbit polyclonal antibody and anti-PD1 rabbit monoclonal antibody, ab228857, Abcam, 1:100) and hematoxylin (AppliChem Inc.) re-staining were performed on the paraffin slices. The routine procedures were according to reports [35, 38]. After the slices were sealed with neutral gum, pathological examination was carried out under Olympus BX53 microscope (Olympus Co.).

2.9. MicroPET imaging

The preparation of PD-L1 antibody labeled with Zirconium-89 ([^{89}Zr] KN035), and its purity and stability *in vitro* were studied by molecular weight exclusion and radioactive high-performance liquid chromatography (radio-HPLC). The *in vitro* stability of the labeled product [^{89}Zr] KN035 was tested, and the radiochemical purity at each time point was used as the reference data of *in vitro* stability. About 400 μL purified [^{89}Zr]KN035 was placed at 4 °C for different time, and its stability in buffer solution was determined by radioactive HPLC. The time points were 6, 24, 48 and 98 h. Then microPET scanning was conducted. Six tumor-bearing mice were selected according to the size and state of the tumor. The microPET scanning method was the same in each group, and the details were as follows: whole body was scanned at 6 different time points after tail vein injection of the tracer, the time points were 4, 24, 48, 72, 96 and 120 h after tracer injection. The animals were placed prone on the scanning bed and anesthetized with 2% isoflurane (oxygen flow rate: 300 mL/min) during the scanning.

In the process of microPET scanning, the detailed information such as animal weight, initial injection dose and measurement time, injection time, residual dose and measurement time, scan time at different time points were recorded accurately on the original recording form. The data of microPET scans were iteratively reconstructed by OSEM 3D method, iteration for twice. The thickness was 0.50 mm, the Matrix was 280 × 280, and the energy window was 350–650 keV.The reconstructed data were analyzed by PMOD software, and the regions of interest (ROIs) were delineated as tumor, heart, liver, kidney and brain. The following for-

mula was used to calculate the percentage of injected dose per gram (% ID/g) values of each organ ROI at different time points.

$$\%ID\,/\,g = \frac{\text{radiouptake in ROI } (\mu Ci/g)}{\text{injection dose } (\mu Ci)} \times 100$$

2.10. Statistical analysis

SPSS 19.0 (SPSS Inc.) software was used for all statistical analysis. The quantitative data were expressed as "mean ± SD". Nonparametric Wilcoxon test was used to evaluate the grade data. T-test was used for the difference comparison between two groups. One-way analysis of variance (one-way ANOVA) was used for the comparison between groups, and repeated-measure sample ANOVA was used to do the variance analysis of repeated measurements. The difference was considered statistically significant when $P < 0.05$.

3. Results

3.1. Identification of CEACAM6 and 4-1BBL gene expression

We have previously demonstrated that transformed SL3261 containing both *CEACAM6* and *4*-1BBL genes can induce transgenic expression of bivalent exogenous antigens *in vivo* and enhance specific and non-specific anti-tumor immune responses, resulting in suppression of tumor growth in experimental CRC model of rats [34, 35]. Construction of the double gene plasmids and identification of the expression of CEACAM6 and 4-1BBL were as follows. 48 h after transfection, the expression of *CEACAM6* and *4*-1BBL genes carried by recombinant plasmids in COS7 cells was detected. COS7 cells transfected by the empty vector plasmid and the recombinant genetic plasmid were identified by RT-PCR. Specific bands of 750–1000 bp (801, 930 bp) were found in the genetically transfected cells by 1% agarose gel electrophoresis under UV light, and there were corresponding specific bands in the positive control group but not in the vector plasmids or negative group (Figure 1A). Previous study also showed that *CEACAM6* and *4*-1BBL genes can be effectively transfected into eukaryotic cells and express antigens successfully [34]. Western blotting assay showed that the recombinant double-gene plasmids were stably expressed in COS7 cells, and Figure 1B shows the molecular weight and abundance of each expressed protein. As shown in Figure 1C, expression of 4-1BBL and CEACAM6 proteins in the intestine and tumor tissues of mice obviously increased after treatment with the bivalent genetic vaccine pIRES-CEACAM6-4-1BBL/SL3261.

3.2. PD-L1 expression in mouse MC38 heterotopic tumor

In order to evaluate whether the MC38 tumor mouse model we established was suitable for anti-PD1/PD-L1 drug therapy, and whether the ^{89}Zr-labeled anti-PD-L1 antibody can be used as a tracer for microPET imaging observation of the tumor model, we examined the expression level of PD-L1 protein in MC38 heterotopic tumor model of mice. As is shown in Figure 2A and B, through both Western blotting and immunohistochemistry assays, we found that the PD-L1 expression in MC38 tumor tissues was very obviously up-regulated when compared with that of the normal tissues (normal tissue samples adjacent to tumor). These results suggest that anti-PD1/PD-L1 drug is suitable for this tumor model, and ^{89}Zr-labeled anti-PD-L1 antibody can be used in the whole-body PET imaging for non-invasive and dynamic observation of this model *in vivo*. As shown in Figure 2C, Western blotting result indicated a low expression of PD-L1 in the intestine, and relatively higher distributions in the heart and liver.

3.2.1. MicroPET imaging of PD-L1 in MC38 heterotopic mice

We used ^{89}Zr-labeled anti-PD-L1 antibody ([^{89}Zr]KN035) as imaging tracer for the whole-body microPET scanning of the mice transplanted with MC38 heterotopic tumor. Representative microPET coronal images of the tumor-bearing mice at different time points are shown in Figure 3A. The PMOD software was used to delineate the regions of interest (ROIs) such as the heart, liver, lung, kidney and tumor, and the scanned data were used to calculate the radiation uptake values (%ID/g, SUV) of the ROIs. The analyzed statistical results of the SUV-mean values (mean ± SD) of several major tissue ROIs at different time points (2, 4, 24, 72, 96, 120 h) are shown in Figure 3B. We found that the uptake of [89Zr]KN035 in tumor tissue (SUV-mean at 4 h, n = 4, 0.631 ± 0.147) was relatively low and was lower than that in the heart (2.876 ± 0.313), liver (2.005 ± 0.098) and kidney (1.761 ± 0.081). This may be related to PD-L1 expression or initial distribution of tracer in blood and metabolic organs. Uptakes in the heart and liver then diminished continuously from the beginning (from 2 h to 120 h). However, the uptake of [^{89}Zr]KN035 in tumor tissue was then accumulated and relatively stable, and it maintained at a higher level after 24 h and lasted at least 120 h (24 h, 1.062 ± 0.182; 72 h, 1.172 ± 0.133; 96 h, 1.065 ± 0.084; 120 h, 1.007 ± 0.132), indicating possible redistribution of radioactive tracer from normal organs to tumor.

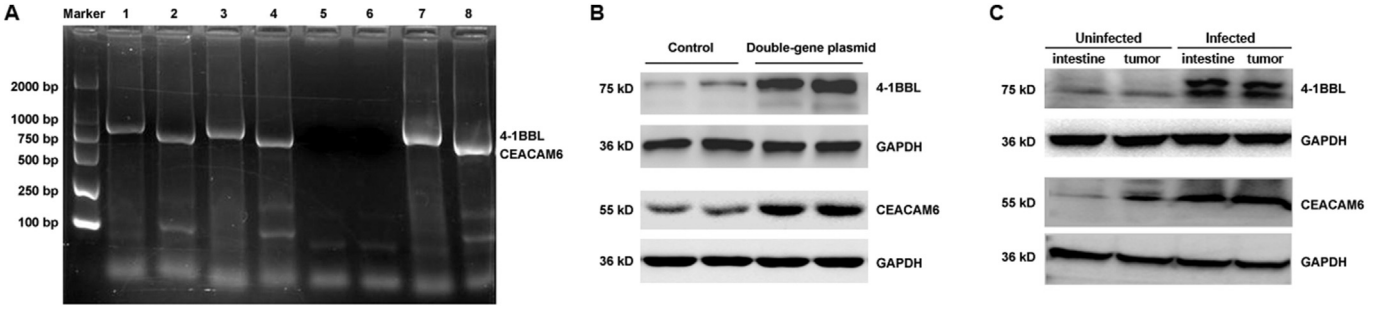

Figure 1. Identification and expression of *CEACAM6/4*-1BBL double genes in COS7 cells. (A) The result of reverse-transcription PCR for identification of CEACAM6/4-1BBL double genes expression in COS7 cells 48 h after transfection. Lane 1, COS7 cells transfected with pIRES-4-1BBL; 2, COS7 cells transfected with pIRES-CEACAM6; 3–4, COS7 cells transfected with pIRES-CEACAM6/4-1BBL; 5, COS7 cells transfected with pIRES vector plasmids; 6, COS7 cells transfected with nothing (negative); 7–8, positive control of pIRES-CEACAM6/4-1BBL plasmids. *4*-1BBL: 930 bp; forward primer: 5-GCTCTAGAGCCACCATGGACCAGCACGCACTTG-3; reverse primer: 5-GGCGGCCGCGTCATCCCTGAGGGGGGTC-3. *CEACAM6*: 801 bp; forward primer: 5-CAGAGCCAAACAACAGAT-3; reverse primer: 5-CATTATTACTTATGCTGACCT-3. Primary uncropped image of (A) is shown in supplementary Figure S1. **(B)** Representative Western blots showing the successful expression of CEACAM6/4-1BBL proteins in COS7 cell line 48 h after transfection. Control: COS7 cells transfected with vector plasmids. Double-gene plasmid: COS7 cells transfected with pIRES-CEACAM6/4-1BBL plasmids. **(C)** Western blotting images showing the expression of 4-1BBL and CEACAM6 proteins in the intestine and tumor tissues of mice treated or not treated with the bivalent genetic vaccine of pIRES-CEACAM6-4-1BBL/SL3261. GAPDH was used as an internal reference. Primary uncropped images of (B) and (C) are shown in supplementary Figure S2.

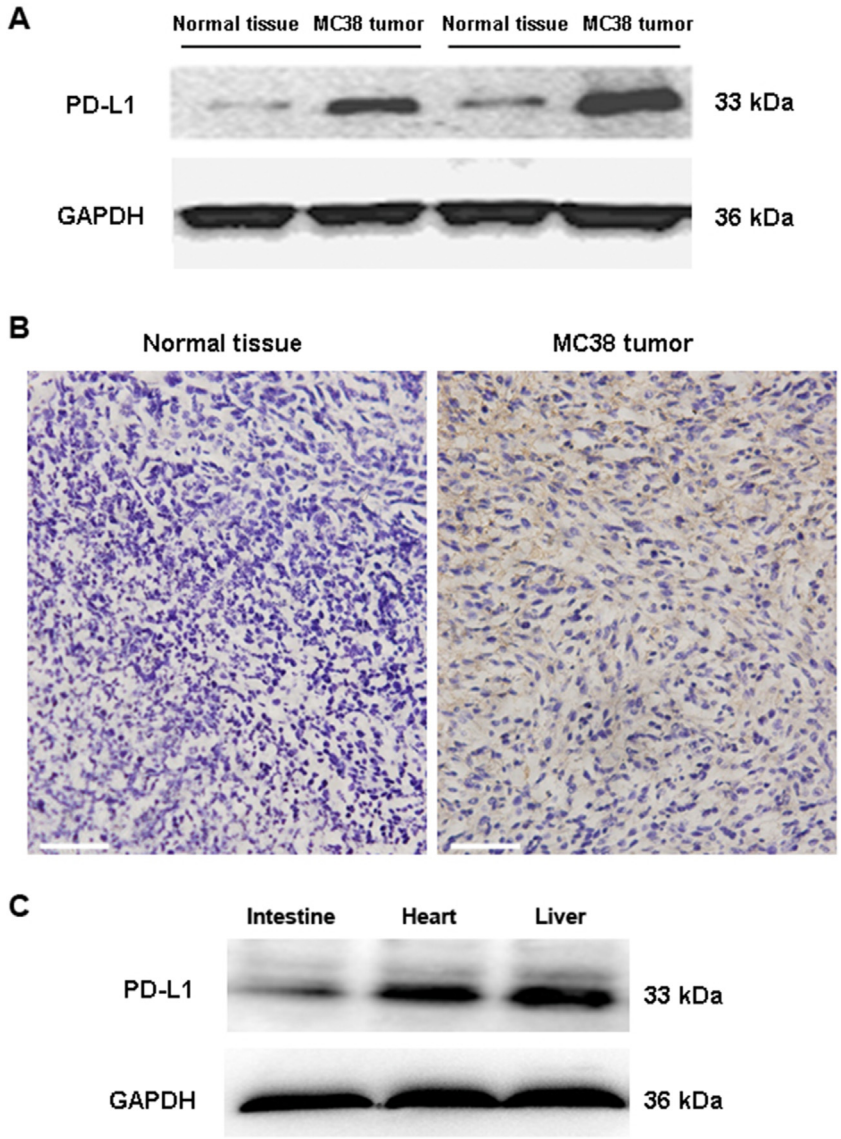

Figure 2. Expression of PD-L1 protein in MC38 tumor tissue of mice. (A) Western blotting result showing the expression of PD-L1 in MC38 tumor tissue and normal tissue from mice 12 days after heterotopic tumor transplantation, which demonstrates overexpression of PD-L1 in MC38 tumor compared with non-tumor tissue. Normal tissue: normal tissue samples adjacent to tumor. MC38 tumor: MC38 heterotopic tumor tissue samples. **(B)** Immunohistochemical assay result showing the expression and distribution of PD-L1 in MC38 tumor tissue. Normal tissue: normal tissue sample adjacent to tumor, which was PD-L1(−). MC38 tumor: MC38 tumor tissue of the model mice, which was PD-L1(+). Purple, hematoxylin staining for cell nucleus; brown, anti-PD-L1 staining. Scale bars, 100 μm. **(C)** Western blots showing the expression of PD-L1 in some normal organs (the intestine, heart, and liver) of mice, which indicated relatively high expression levels of PD-L1 in the heart and liver. Primary uncropped images of (A) and (C) are shown in supplementary Figure S3.

4. Efficacy of PD1 antibody in combination with CEACAM6/4-1BBL vaccine

Then we examined the efficacy of the therapeutical combination of pIRES-CEACAM6-4-1BBL/SL3261 vaccine and anti-PD1 antibody Nivolumab (20 mg/kg in mice). Treatments and observation were started from 14 days after the MC38 heterotopic tumor transplantation injection. We investigated the tumor development of the treated group mice by tumor volume evaluation, [^{89}Zr]KN035 PET imaging, and assessment of immunohistochemical indicators. As is shown in Figure 4A, we found that the tumor volumes of the vaccine alone group grew slower than that of the control group during the first several days, but the gap between the two groups got narrowed in the following days, and there was no significant difference between the two groups considering time factor ($p = 0.165$). However, the tumor volume growth of the combined immunotherapy group mice was almost totally suppressed during the entire 12-day observation period ($p < 0.001$ vs. control, $p = 0.048$ vs. vaccine group) (total comparison result of the three groups by repeated-measure sample ANOVA, $F = 45.794$, $p = 0.000232$; $n = 4$ mice for each group). Figure 4B shows the representative isolated xenograft MC38 tumors of the control (2490 mm^3), vaccine (2147), and combined immunotherapy (1181) groups. This result suggests that the combined immunotherapy has dramatic improvement in antitumor effectiveness.

4.1. Drug efficacy of combined immunotherapy imaged by [^{89}Zr]KN035 PET

After 14 days of treatment, we investigated the tumor radioactive uptake by microPET imaging with the formerly used tracer [^{89}Zr]KN035. The representative microPET images before and after tumor immunotherapeutic treatment with the bivalent genetic vaccine and anti-PD1 antibody are shown in Figure 5A. We calculated and compared the normal tissues and tumor uptake values (%ID/g, SUV) of the model mice to evaluate effect of the combined immunotherapy on tumor development. As is shown in Figure 5B, the radioactive uptake (SUV-mean) of the tumor area ROIs was significantly decreased after 14 days of treatment with the combination of pIRES-CEACAM6-4-1BBL/SL3261 vaccine and anti-PD1 antibody Nivolumab ($n = 4$ for each group; SUV-mean at time point of 24 h: pre-treatment, 1.141 ± 0.168; post-treatment, 0.415 ± 0.104, $P = 0.006$ vs. pre-treatment), indicating the efficacy of the combined therapy for MC38 tumor. There were also significant differences in the lung (48 h: pre-treatment,

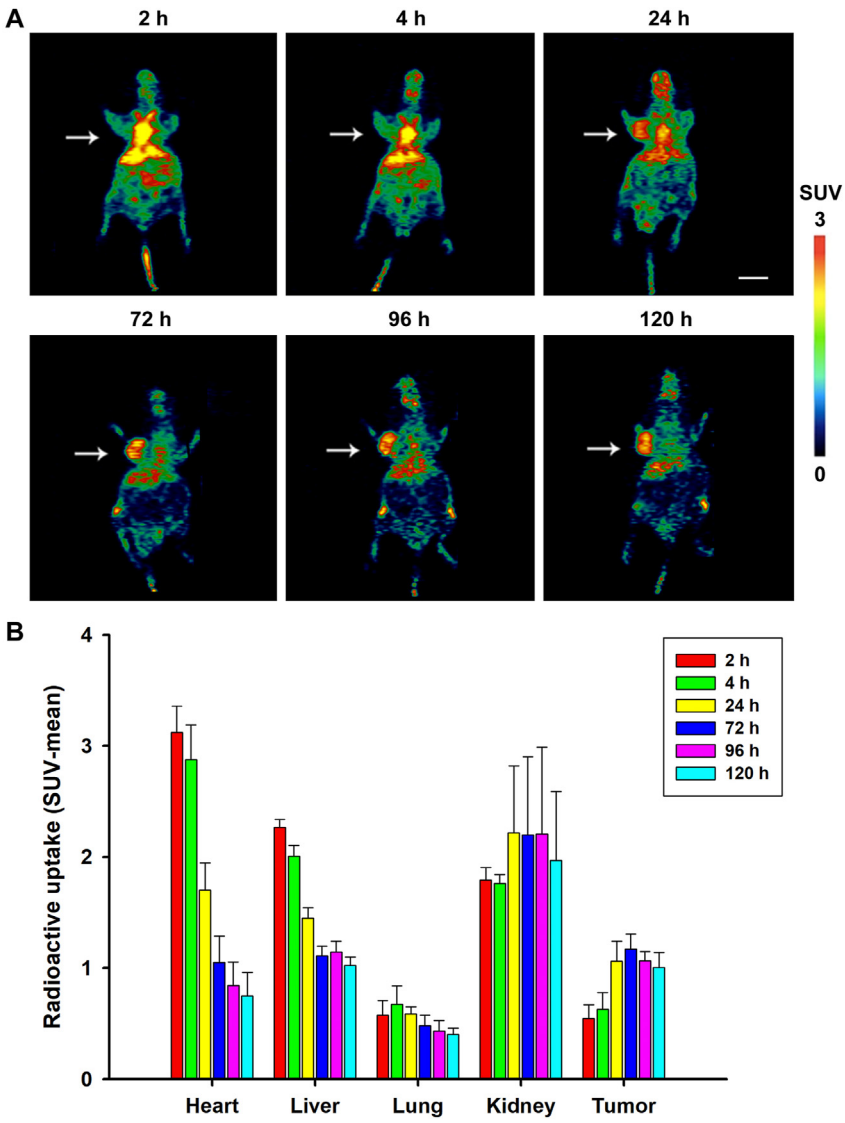

Figure 3. MicroPET imaging with [^{89}Zr] KN035 in MC38 tumor model mice. (A) Representative [^{89}Zr]KN035 PET imaging results showing the dynamic distribution of PD-L1 in mice at different time points after tracer injection from 1 week post-transplantation. [^{89}Zr]KN035, ^{89}Zr-labeled anti-PD-L1 antibody KN035. Arrows, heterotopic tumors; scale bar, 1 cm. **(B)** Statistical results of the radioactive uptake of [^{89}Zr] KN035 and PD-L1 distribution in different regions of interest (ROIs) at several time points after injection in mice (n = 4). SUV-mean, mean standard radioactive uptake values.

0.594 ± 0.077; post-treatment, 0.880 ± 0.085, P = 0.018) and especially in the liver (96 h: pre-treatment, 1.179 ± 0.039; post-treatment, 1.609 ± 0.112, P = 0.0007) between pre-treatment and post-treatment. These changes may be related to the pathology, therapy and metabolic state of the mice.

4.2. Changed PD1/PD-L1 expression in tumor tissues after genetic immunotherapy

We also examined the tumor development in mouse model by means of assessment of tumor biochemical indicators, such as PD1 and PD-L1. The expression of PD1/PD-L1 immunocheckpoint proteins is an important biomarker for the applicability of anti-tumor immunotherapy and tumor drug resistance. As shown in Figure 6A and B, after treatment for 14 days, the expression of PD1/PD-L1, especially PD1, was up-regulated by the treatment with vaccine alone in the MC38 tumor tissue of the model mice, but the expression levels of PD1 and PD-L1 in the combined therapy group were significantly lower than the vaccine alone group (Figure 6B; mean integral optical density of PD1: Control, 7.2993 ± 0.5763; Vaccine alone, 19.6617 ± 3.1214, P < 0.001 vs. Control; Combined therapy, 5.192 ± 0.4405, P < 0.001 vs. Vaccine alone. PD-L1: Control, 12.094 ± 1.1753; Vaccine alone, 15.6423 ± 2.445, P = 0.039 vs. Control; Combined therapy, 11.7043 ± 1.8761, P = 0.045 vs. Vaccine alone; n = 3). These results suggest that combined immunotherapy with anti-PD1 drugs may reduce drug resistance of tumor and expand the range of indications.

5. Discussion

In this study, we constructed eukaryotic expression vector carrying *CEACAM6/4*-1BBL genes and introduced it into attenuated SL3261 to obtain a stable transformation strain. In order to explore the anti-tumor efficacy of this bivalent attenuated SL3261 vaccine combined with PD1 inhibitory antibody, MC38 cell line was used to establish a heterotopic tumor-bearing mouse model, and the anti-tumor immune function and anti-tumor therapeutic effect of the combined immunotherapy on mice were studied. The expression of PD-L1 in tumor tissue was detected by PET/CT imaging with [^{89}Zr]KN035 as tracer before and after treatment in all experimental animals, and the expression of PD-L1 and PD1 was also detected by Western blots and IHC. This study, together with our previous findings, preliminarily proves that this new combined immunotherapy can enhance the cellular immune function of the body and inhibit the growth of CRC tumor, and provides experimental and theoretical basis for the application of *CEACAM6* and *4*-1BBL bivalent genetic vaccine transfection and combined anti-tumor immunotherapy in the treatment of CRC.

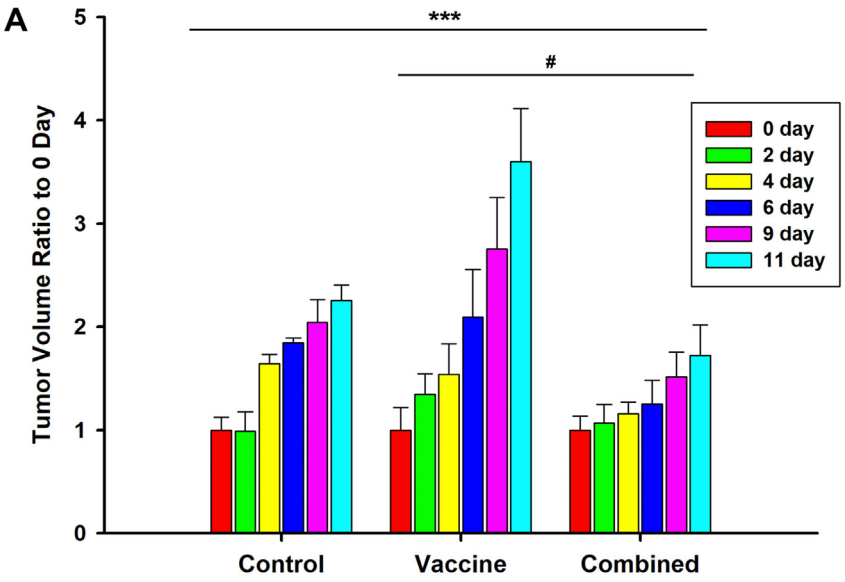

Figure 4. Drug efficacy of anti-PD1 antibody combined with *CEACAM6/4*-1BBL genetic vaccine. (A) Statistical result of the therapeutical effect of CEACAM6/4-1BBL vaccine, and PD1 antibody (Nivolumab) combined with vaccine, on the growth of MC38 heterotopic tumor in mice (averages of tumor volume ratios, and SD). Treatments started at 2 weeks after heterotopic tumor transplantation. Control, given vehicle. Vaccine, given the bivalent vaccine of pIRES-CEACAM6-4-1BBL/SL3261 alone. Combined, treated with bivalent vaccine and PD1 antibody (Nivolumab, 20 mg/kg) together. **(B)** Representative images of isolated MC38 tumors of the control (2490 mm^3), vaccine (2147), and combined immunotherapy (1181) groups. N = 4 per time point. ***P < 0.001, Combined vs. Control; #P < 0.05, Combined vs. Vaccine.

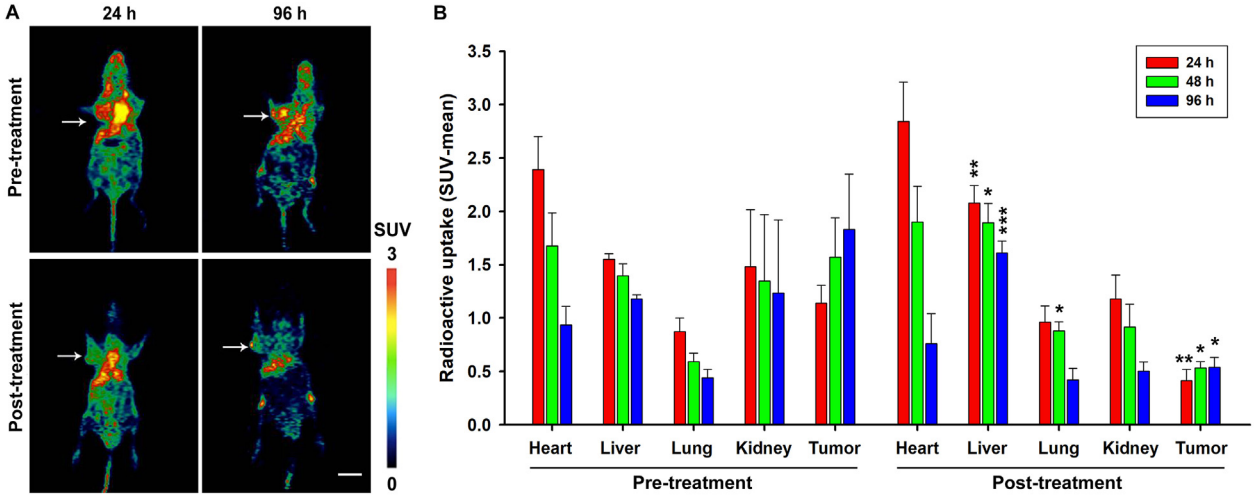

Figure 5. Anti-tumor efficacy of the combined immunotherapy imaged by [^{89}Zr] KN035 PET. (A) Representative microPET imaging results of the MC38 heterotopic tumor mice with [^{89}Zr]KN035, showing the decrease in tumor [^{89}Zr]KN035 uptake and reduced areas of heterotopic tumor. Pre-treatment group, injected with tracer after 7 days of heterotopic tumor modeling, and PET scanned at 24 h, 48 h and 96 h after tracer injection. Post-treatment, scanned at the same time points post tracer injection after 14 days of combined treatment. Arrows, heterotopic tumors; scale bar, 1 cm. **(B)** Statistical result about the effect of the combined immunotherapy on tumor tissue radioactive uptake by [^{89}Zr]KN035 PET imaging. SUV-mean, mean standard radioactive uptake value. N = 4 per group. *P < 0.05, **P < 0.01, and ***P < 0.001 vs. Pre-treatment.

Our previous studies have demonstrated that attenuated SL3261 containing *CEACAM6/4*-1BBL genes given via gastric lavage can express the recombinant proteins in CRC model animals and increase the activity and invasion to tumor tissues of CD3+, CD8+ T cells and natural killer (NK) cells, decrease the infiltration of regulatory T cells and the number of Foxp3+ T cells, promote Th1 polarization and inhibit Th2 and Th17

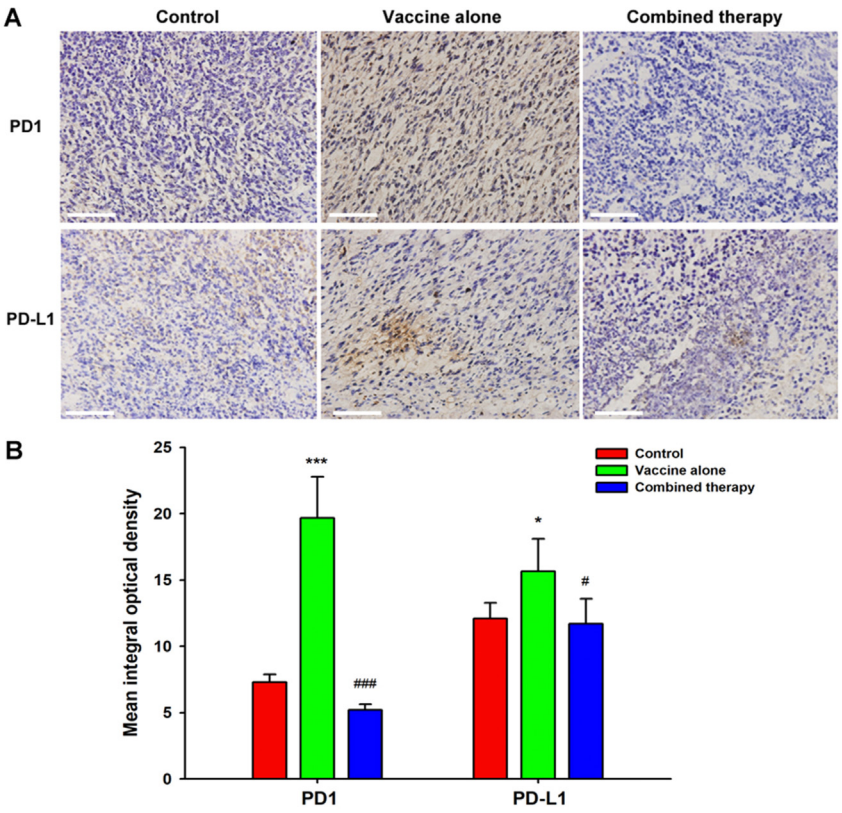

Figure 6. Tumor tissue PD1/PD-L1 expression after treatment with *CEACAM6/4*-1BBL vaccine and anti-PD1 immunotherapy. (A) Representative immunohistochemical images showing the expression of PD-1 and PD-L1 in MC38 tumor tissue after treatment. Control, given vehicle; Vaccine alone, given the bivalent vaccine; Combined immunotherapy, given bivalent vaccine and anti-PD1 drug (Nivolumab). Tissue samples were collected at 2 weeks after treatments. Purple, hematoxylin staining for nucleus; brown, anti-PD1 or anti-PD-L1 staining. Scale bars, 100 μm. **(B)** Statistical results of the mean integral optical density (MIOD, IOD/Area) of the IHC images. N = 3 per group. *P < 0.05, ***P < 0.001 vs. Control; #P < 0.05, ###P < 0.001 vs. Vaccine alone.

polarization, producing specific and non-specific anti-tumor immune responses and inhibiting the growth of colorectal tumor [34, 35]. PD1 inhibitors, as immunotherapy drugs, have been used in clinical practice and have a clear effect on specific tumors, which provides a basis for combined immunotherapy. In accordance with the previous research results, this study found that the bivalent genetic vaccine SL3261 can effectively transfer foreign genes into eukaryotic cells and express proteins. This gene vaccine can inhibit tumor growth, and the effect is stronger when combined with anti-PD1 drugs. Our *in vitro* expression and identification of the recombinant pIRES-CEACAM6-4-1BBL eukaryotic expression vector was as previous. The pIRES-CEACAM6-4-1BBL plasmid was transfected into COS7 cells by liposome and the cells and culture supernatant were harvested on the third day, and RT-PCR was used to examine the transcription of target genes in transfected cells and WB assay was used to detect the expression of CEACAM6 and 4-1BBL in the culture supernatants. Our experiments proved that bivalent attenuated SL3261 vaccine containing eukaryotic expression plasmids can inhibit CRC and MC38 tumor growth by enhancing anti-tumor cell immunity and breaking the immunosuppressive microenvironment [34, 35].

Previous research has revealed part of the immunological mechanism for the bivalent vaccine against CRC, and we can draw consistent conclusions from this study. At the same time, we found that the gene vaccine treatment could increase the expression of PD1, perhaps in a compensatory manner. It may promote tumor immune escape and tolerance to immunotherapy, and on the other hand, it may also convert “cold” tumor to “hot” tumor, which provides a prerequisite for the effectiveness of tumor immunotherapy such as PD1 inhibitors. The results of this study provide a theoretical basis and a reasonable explanation for the efficacy of anti-PD1 drugs combined with bivalent genetic vaccineSL3261. *Salmonella* is a Gram-negative bacterium and anaerobe, and is itself a natural immune adjuvant that can induce inflammatory response and enhance immune function. Whereas tumor tissue is rich in nutrients and metabolically robust, and additionally the rapid growth of tumor leads to a lack of local blood supply and an anaerobic area, these enable *Salmonella* to accumulate and proliferate in tumor tissue [39]. In addition, *Salmonella* has a direct tumor-lytic effect, and attenuated strains have a better targeted colonization to antigen presenting cells (APCs) [40, 41]. Exogenous genes with attenuated *Salmonella typhimurium* as vector can selectively express proteins in APCs (including macrophages, dendritic cells) and tumor tissues to enhance specific and non-specific immunity against tumor. Therefore, the genetic vaccine carried by attenuated SL3261 has obvious advantages in anti-tumor genetic immunotherapy.

Clinical studies have shown that only highly microsatellite-instable (MSI-H) CRC patients could benefit from immunocheckpoint inhibitors and these patients only occupy 10% in patients with metastatic CRC, but 90% of the non-MSI-H (MSS/MSI-L) patients cannot benefit from drugs such as PD1 inhibitors [42, 43]. The reasons for this may be that non-MSI-H CRC belongs to “non-immunogenic tumor” and it cannot stimulate anti-tumor immune response, and that the efficacy of PD1 does not last long and is limited in practical clinical application. Studies have shown that the benefits of checkpoint inhibitors come from a short revival of depleted T cells, not a permanent change in their state [44]. Even if the PD-1 inhibition is maintained, these tumor-specific T cells still need "fuel" to proliferate and restore effective immune responses. The fuel comes from co-stimulation based on CD28 molecules. Thus, CD28 on the surface of T cells may be a clinical biomarker that can predict the efficacy of anti-PD1 drugs [45]. Efficient means to change a non-immunogenic tumor to an immunogenic “hot tumor” is combined therapy, which has complementary anti-tumor immune effects, including blockade of the inhibitory signals and activation of the co-stimulatory signals [46, 47]. PD1 is a critical component in the activation of immune T cells, so PD1 axis inhibitors should be the cornerstone of anti-tumor combined therapy. Based on the complementary effects for T cell activation, drugs such as 4-1BB agonists, indoleamine 2,3-dioxygenase inhibitors [48] and antibody drugs are also potential combination drugs. Our therapeutic efficacy study found that the effect of combined immunotherapy was significantly improved compared with the genetic immunotherapy.

Combined immunotherapy, especially targeting at different immunocheckpoints, can better improve the antitumor immune response and become a promising treatment option [49, 50]. Studies have shown that targeted therapy combined with multiple immunocheckpoint blockers can provide long-term antitumor immunity and improve treatment outcomes in patients with melanoma and non-small cell lung cancer [51, 52, 53]. Blocking both CTLA-4 and PD-L1 can increase anti-tumor immune activity in IL-15-dependent manner in a mouse model of metastatic CT26 intestinal cancer [54]. The immune system can control the malignant transformation of cells, which often occurs in the body. According to the theory of "immune editing", the immune system can also reshape tumor, which includes three stages: immune elimination, immune balance and immune escape [55, 56, 57]. Tumor cells can escape from immune surveillance in many ways, such as deficiency or low expression of tumor-associated antigens, abnormal antigen presentation, lack of co-stimulatory signals, T cell incompetence, and abnormal expression of cytokines. In the study of myeloma, it was found that the CEACAM6 protein on the surface of myeloma cells could bind and cross-link with cytotoxic T lymphocyte (CTL), thus weakening the activity and causing nonreactivity of T cells. Neutralizing the CEACAM6 protein with specific monoclonal antibody or silencing the *CEACAM6* gene with siRNA, the T cells can resume their normal immune response to tumor cells [58]. Accumulating studies have shown that, in addition to secondary lymphoid tissues, anti-tumor immunity also occurs in the tertiary lymphoid structures (TLSs) within the tumor, thus restoring the function of TLSs and its lymphocytes is a promising strategy of antitumor immunotherapy [59]. 4-1BB is expressed in many lymphoid cells and its agonists including 4-1BBL induce important co-stimulatory signals and strong antitumor immune responses [25, 26]. This may explain why the combined immunotherapy with bivalent genetic vaccine and immunocheckpoint blocker in this study has better antitumor effect in MC38 animal models.

In clinical trials for lung cancer, patients with high expression of PD-L1 showed better response to PD1 inhibitors [60]. But how to non-invasively and precisely predict tumor response to PD1 inhibitors, thus reducing unnecessary drug use and promoting accurate treatment, is also a problem to be considered. As a non-invasive molecular imaging method, PET can reflect tumor progression through biological process, and is also a new quantitative detection method. Small animal PET (microPET) was designed for the study of human diseases in animal models [61]. PET can be used for continuous longitudinal study on the same subject to obtain the whole data of all time points, and realize non-invasive, dynamic and quantitative observation of physiological and pathological changes *in vivo*, which can be used to effectively study the pathogenesis of diseases and is of great value in the evaluation of curative effect of treatments [62, 63]. Previous studies have shown that using ^{89}Zr-labeled PD-L1 antibody (KN035) as a tracer, microPET imaging of the whole body after tail vein injection can accurately identify the expression of PD-L1 in tumor tissues, thus providing real-time, non-invasive guidance for drug use and monitoring of therapeutic effect [64]. In this study, we also observed clear and definite results of PET imaging with this tracer in MC38 tumor-bearing mice. Moreover, due to the requirement for combination therapy, we need not only to find reliable predictors for the use of PD1 inhibitors, but also to be alert to possible side effects of combined therapies, and therefore, preclinical transformation research in animal models is very important.

Tumor microenvironment is usually immunosuppressive, so it is a pivotal strategy of tumor immunotherapy to overcome the suppressive microenvironment by combining immunocheckpoint inhibitors and tumor vaccine drugs [65]. In accordance with our previous work, we transfected the *CEACAM6* and *4*-1BBL genes into APCs *in vivo* using SL3261 vector, and this enhanced the specific (CEACAM6) and non-specific anti-tumor immunity (4-1BBL). This method provides a new strategy for the study of *in vivo* APC transfection of tumor-associated antigen and co-stimulatory molecule genes, and may become a new approach for the treatment of CRC. Although there are many forms of CEA vaccine, CEA cannot successfully stimulate the production of effective anti-tumor response due to the possibility of immune tolerance to CEA and the reduction of immune function in tumor-bearing state [16, 66]. After constructing eukaryotic expression plasmid containing both *CEACAM6* and *4*-1BBL genes, we gave the attenuated *Salmonella typhimurium* carrying the double genes to MC38 tumor model mice, and with the combination of PD1 inhibitor, we found that this combined therapy can enhance the antitumor immune function and improve the therapeutic effect on CRC. In addition, micoPET/CT imaging with [^{89}Zr] KN035 was successfully used to monitor the expression of PD-L1 in tumor tissue and assess the efficacy of combined immunotherapy. Activating immune system may lead to immune overdrive, such as cytokine storms, which can have severe adverse effects. It has also been reported that overexpression of 4-1BB/4-1BBL may be one of the causes of arteriosclerosis [67], even though we did not see any difference in the physical appearance of the mice that were given the bivalent vaccine compared to the control group. How to make sure that the expression level of genetic vaccine after transfection can be kept in a moderate range, which can not only enhance the antitumor immune response, but also avoid obvious adverse reaction, will become a major issue for future clinical application, and this needs further and more detailed studies.

In summary, in this study, the eukaryotic expression plasmid containing *CEACAM6/4*-1BBL genes, which had been successfully constructed in our previous studies, was introduced into the attenuated SL3261 and stable transformed strain was obtained. The results show that the bivalent genetic vaccine combined with PD1 inhibitor can enhance the antitumor immune function and inhibit the growth of tumor, and this provides support for DNA vaccine intervention combined with immunotherapy for cancer therapy. By overcoming the immune tolerance and suppressive microenvironment, and inhibiting the immune brake induced by immunocheckpoint activation, this combined immunotherapy can effectively inhibit the growth of MC38 tumor, and provide experimental and theoretical basis for curing CRC with genetic vaccine and traditional immunotherapy.

Declarations

Author contribution statement

Yuzhen Li: Analyzed and interpreted the data; Wrote the paper.

Xiaodan Zhu: Conceived and designed the experiments; Performed the experiments.

Chunhui Jin: Conceived and designed the experiments.

Jianliang You: Performed the experiments.

Baonan Zhang: Analyzed and interpreted the data.

Xiaona Huang: Contributed reagents, materials, analysis tools or data.

Funding statement

Dr. Chunhui Jin was supported by the Science and Education Strong Health Project of Wuxi Municipal Health Commission [ZDYCPR011].

Data availability statement

Data included in article/supp. material/referenced in article.

Declaration of interest's statement

The authors declare no conflict of interest.

Additional information

Supplementary content related to this article has been published online at https://doi.org/10.1016/j.heliyon.2022.e10775.

References

[1] W. Chen, R. Zheng, P.D. Baade, S. Zhang, H. Zeng, F. Bray, et al., Cancer statistics in China, 2015, CA 66 (2) (2016) 115–132.

[2] P. Correale, C. Botta, D. Ciliberto, P. Pastina, R. Ingargiola, S. Zappavigna, et al., Immunotherapy of colorectal cancer: new perspectives after a long path, Immunotherapy 8 (11) (2016) 1281–1292.

[3] R. Siegel, D. Naishadham, A. Jemal, Cancer statistics, 2013, CA 63 (1) (2013) 11–30.

[4] A. Nappi, M. Berretta, C. Romano, S. Tafuto, A. Cassata, R. Casaretti, et al., Metastatic colorectal cancer: role of target therapies and future perspectives, Curr. Cancer Drug Targ. 18 (5) (2018) 421–429.

[5] I.S. Woo, Y.H. Jung, Metronomic chemotherapy in metastatic colorectal cancer, Cancer Lett. 400 (2017) 319–324.

[6] S. Koido, S. Homma, A. Takahara, Y. Namiki, S. Tsukinaga, J. Mitobe, et al., Current immunotherapeutic approaches in pancreatic cancer, Clin. Dev. Immunol. 2011 (2011), 267539. PubMed PMID: 21922022; PubMed Central PMCID: PMCPMC3172984.

[7] D. Weng, B. Song, S. Koido, S.K. Calderwood, J. Gong, Immunotherapy of radioresistant mammary tumors with early metastasis using molecular chaperone vaccines combined with ionizing radiation, J. Immunol. 191 (2) (2013) 755–763. PubMed PMID: 23772032; PubMed Central PMCID: PMCPMC4085737.

[8] J. Ge, L. Zhu, J. Zhou, G. Li, Y. Li, S. Li, et al., Association between co-inhibitory molecule gene tagging single nucleotide polymorphisms and the risk of colorectal cancer in Chinese, J. Cancer Res. Clin. Oncol. 141 (9) (2015) 1533–1544. PubMed PMID: 25604582.

[9] Z. Mojtahedi, M. Mohmedi, S. Rahimifar, N. Erfani, S.V. Hosseini, A. Ghaderi, Programmed death-1 gene polymorphism (PD-1.5 C/T) is associated with colon cancer, Gene 508 (2) (2012) 229–232. PubMed PMID: 22892379.

[10] P.P. Singh, P.K. Sharma, G. Krishnan, A.C. Lockhart, Immune checkpoints and immunotherapy for colorectal cancer, Gastroenterology report 3 (4) (2015) 289–297. PubMed PMID: 26510455; PubMed Central PMCID: PMCPMC4650981.

[11] S. Mocellin, C.R. Rossi, M. Lise, F.M. Marincola, Adjuvant immunotherapy for solid tumors: from promise to clinical application, Cancer Immunol. Immunother. 51 (11-12) (2002) 583–595. PubMed PMID: 12439603.

[12] D.M. Pardoll, Spinning molecular immunology into successful immunotherapy, Nat. Rev. Immunol. 2 (4) (2002) 227–238. PubMed PMID: 12001994.

[13] M.E. Gatti-Mays, J.M. Redman, J.M. Collins, M. Bilusic, Cancer vaccines: enhanced immunogenic modulation through therapeutic combinations, Hum. Vaccines Immunother. 13 (11) (2017) 2561–2574. PubMed PMID: 28857666; PubMed Central PMCID: PMCPMC5703410.

[14] W. Zhang, S. Wang, J. Gu, Y. Gao, Z. Wang, K. Zhang, et al., Synergistic tumoricidal effect of combined hPD-L1 vaccine and HER2 gene vaccine, Biochem. Biophys. Res. Commun. 497 (1) (2018) 394–400. PubMed PMID: 29438713.

[15] S. Loisel-Meyer, T. Felizardo, J. Mariotti, M.E. Mossoba, J.E. Foley, R. Kammerer, et al., Potent induction of B- and T-cell immunity against human carcinoembryonic antigen-expressing tumors in human carcinoembryonic antigen transgenic mice mediated by direct lentivector injection, Mol. Cancer Therapeut. 8 (3) (2009) 692–702. PubMed PMID: 19276164; PubMed Central PMCID: PMCPMC2846382.

[16] J.A. Hensel, V. Khattar, R. Ashton, S. Ponnazhagan, Recombinant AAV-CEA tumor vaccine in combination with an immune adjuvant breaks tolerance and provides protective immunity, Mol. Ther. Oncolyt. 12 (2019) 41–48. PubMed PMID: 30666318; PubMed Central PMCID: PMCPMC6329706.

[17] S. Cameron, L.M. de Long, M. Hazar-Rethinam, E. Topkas, L. Endo-Munoz, A. Cumming, et al., Focal overexpression of CEACAM6 contributes to enhanced tumourigenesis in head and neck cancer via suppression of apoptosis, Mol. Cancer 11 (2012) 74. PubMed PMID: 23021083; PubMed Central PMCID: PMCPMC3515475.

[18] M.L. Taddei, E. Giannoni, T. Fiaschi, P. Chiarugi, Anoikis: an emerging hallmark in health and diseases, J. Pathol. 226 (2) (2012) 380–393. PubMed PMID: 21953325.

[19] J.S. Lewis-Wambi, H.E. Cunliffe, H.R. Kim, A.L. Willis, V.C. Jordan, Overexpression of CEACAM6 promotes migration and invasion of oestrogen-deprived breast cancer cells, Eur. J. Cancer 44 (12) (2008) 1770–1779. PubMed PMID: 18614350; PubMed Central PMCID: PMCPMC2778047.

[20] R. Holmer, G.H. Wätzig, S. Tiwari, S. Rose-John, H. Kalthoff, Interleukin-6 trans-signaling increases the expression of carcinoembryonic antigen-related cell adhesion molecules 5 and 6 in colorectal cancer cells, BMC Cancer 15 (2015) 975. PubMed PMID: 26673628; PubMed Central PMCID: PMCPMC4682226.

[21] K.S. Kim, J.T. Kim, S.J. Lee, M.A. Kang, I.S. Choe, Y.H. Kang, et al., Overexpression and clinical significance of carcinoembryonic antigen-related cell adhesion molecule 6 in colorectal cancer, Clinica Chim. Acta 415 (2013) 12–19. PubMed PMID: 22975528.

[22] M.R. Alderson, C.A. Smith, T.W. Tough, T. Davis-Smith, R.J. Armitage, B. Falk, et al., Molecular and biological characterization of human 4-1BB and its ligand, Eur. J. Immunol. 24 (9) (1994) 2219–2227. PubMed PMID: 8088337.

[23] J.L. Cannons, P. Lau, B. Ghumman, M.A. DeBenedette, H. Yagita, K. Okumura, et al., 4-1BB ligand induces cell division, sustains survival, and enhances effector function of CD4 and CD8 T cells with similar efficacy, J. Immunol. 167 (3) (2001) 1313–1324. PubMed PMID: 11466348.

[24] C. Wang, G.H. Lin, A.J. McPherson, T.H. Watts, Immune regulation by 4-1BB and 4-1BBL: complexities and challenges, Immunol. Rev. 229 (1) (2009) 192–215. PubMed PMID: 19426223.

[25] J.M. Zapata, G. Perez-Chacon, P. Carr-Baena, I. Martinez-Forero, A. Azpilikueta, I. Otano, et al., CD137 (4-1BB) signalosome: complexity is a matter of TRAFs, Front. Immunol. 9 (2018) 2618. PubMed PMID: 30524423; PubMed Central PMCID: PMCPMC6262405.

[26] I. Etxeberria, J. Glez-Vaz, Á. Teijeira, I. Melero, New emerging targets in cancer immunotherapy: CD137/4-1BB costimulatory axis, ESMO open 4 (3) (2020), e000733. PubMed PMID: 32611557; PubMed Central PMCID: PMCPMC7333812.

[27] D. Cepowicz, M. Gryko, K. Zaręba, A. Stasiak-Bermuta, B. Kędra, Assessment of activity of an adhesion molecule CD134 and CD137 in colorectal cancer patients, Pol. Przegl. Chir. 83 (12) (2011) 641–645. PubMed PMID: 22343199.

[28] J.X. Ye, Y.T. Zhang, X.G. Zhang, D.M. Ren, W.C. Chen, Recombinant attenuated Salmonella harboring 4-1BB ligand gene enhances cellular immunity, Vaccine 27 (11) (2009) 1717–1723. PubMed PMID: 19187795.

[29] J. Ye, L. Li, Y. Zhang, X. Zhang, D. Ren, W. Chen, Recombinant Salmonella-based 4-1BBL vaccine enhances T cell immunity and inhibits the development of colorectal cancer in rats: in vivo effects of vaccine containing 4-1BBL, J. Biomed. Sci. 20 (1) (2013) 8. PubMed PMID: 23413971; PubMed Central PMCID: PMCPMC3605352.

[30] X.L. Zhang, V.T. Jeza, Q. Pan, Salmonella typhi: from a human pathogen to a vaccine vector, Cell. Mol. Immunol. 5 (2) (2008) 91–97. PubMed PMID: 18445338; PubMed Central PMCID: PMCPMC4651240.

[31] X. Xu, W.A. Hegazy, L. Guo, X. Gao, A.N. Courtney, S. Kurbanov, et al., Effective cancer vaccine platform based on attenuated salmonella and a type III secretion system, Cancer Res. 74 (21) (2014) 6260–6270. PubMed PMID: 25213323; PubMed Central PMCID: PMCPMC4216746.

[32] J.Z. Meng, Y.J. Dong, H. Huang, S. Li, Y. Zhong, S.L. Liu, et al., Oral vaccination with attenuated Salmonella enterica strains encoding T-cell epitopes from tumor antigen NY-ESO-1 induces specific cytotoxic T-lymphocyte responses, Clin. Vaccine Immunol. : CVI 17 (6) (2010) 889–894. PubMed PMID: 20375244; PubMed Central PMCID: PMCPMC2884430.

[33] K. Liang, Q. Liu, P. Li, H. Luo, H. Wang, Q. Kong, Genetically engineered Salmonella Typhimurium: recent advances in cancer therapy, Cancer Lett. 448 (2019) 168–181. PubMed PMID: 30753837.

[34] C. Jin, Y. Liu, J. Zhu, T. Xia, B. Zhang, Y. Fei, et al., Recombinant Salmonella-based CEACAM6 and 4-1BBL vaccine enhances T-cell immunity and inhibits the development of colorectal cancer in rats: in vivo effects of vaccine containing 4-1BBL and CEACAM6, Oncol. Rep. 33 (6) (2015) 2837–2844. PubMed PMID: 25872647.

[35] C. Jin, X. Duan, Y. Liu, J. Zhu, K. Zhang, Y. Zhang, et al., T cell immunity induced by a bivalent Salmonella-based CEACAM6 and 4-1BBL vaccines in a rat colorectal cancer model, Oncol. Lett. 13 (5) (2017) 3753–3759. PubMed PMID: 28521477; PubMed Central PMCID: PMCPMC5431390.

[36] N. Grobe, M. Di Fulvio, N. Kashkari, H. Chodavarapu, H.K. Somineni, R. Singh, et al., Functional and molecular evidence for expression of the renin angiotensin system and ADAM17-mediated ACE2 shedding in COS7 cells, Am. J. Physiol. Cell Physiol. 308 (9) (2015) C767–C777.

[37] W. Liu, S. Wang, Q. Sun, Z. Yang, M. Liu, H. Tang, DCLK1 promotes epithelial-mesenchymal transition via the PI3K/Akt/NF-κB pathway in colorectal cancer, Int. J. Cancer 142 (10) (2018) 2068–2079. PubMed PMID: 29277893.

[38] J. McLaughlin, G. Han, K.A. Schalper, D. Carvajal-Hausdorf, V. Pelekanou, J. Rehman, et al., Quantitative assessment of the heterogeneity of PD-L1 expression in non-small-cell lung cancer, JAMA Oncol. 2 (1) (2016) 46–54. PubMed PMID: 26562159; PubMed Central PMCID: PMCPMC4941982.

[39] W. Yoon, Y. Yoo, Y.S. Chae, S.H. Kee, B.M. Kim, Therapeutic advantage of genetically engineered Salmonella typhimurium carrying short hairpin RNA against inhibin alpha subunit in cancer treatment, Ann. Oncol 29 (9) (2018) 2010–2017. PubMed PMID: 30016386.

[40] A. Vendrell, M.J. Gravisaco, J.C. Goin, M.F. Pasetti, L. Herschllik, J. De Toro, et al., Therapeutic effects of Salmonella typhi in a mouse model of T-cell lymphoma, J. Immun. 36 (3) (2013) 171–180. PubMed PMID: 23502764.

[41] T.J. Wilson, S. Clare, J. Mikulin, C.M. Johnson, K. Harcourt, P.A. Lyons, et al., Signalling lymphocyte activation molecule family member 9 is found on select subsets of antigen-presenting cells and promotes resistance to Salmonella infection, Immunology 159 (4) (2020) 393–403. PubMed PMID: 31880316; PubMed Central PMCID: PMCPMC7078004.

[42] K.M. Smith, J. Desai, Nivolumab for the treatment of colorectal cancer, Expet Rev. Anticancer Ther. 18 (7) (2018) 611–618. PubMed PMID: 29792730.

[43] S. Inoue, H. Ito, T. Tsunoda, H. Murakami, M. Ebi, N. Ogasawara, et al., CD70 expression in tumor-associated fibroblasts predicts worse survival in colorectal cancer patients, Virchows Arch. 475 (4) (2019) 425–434. PubMed PMID: 30980190.

[44] K.E. Pauken, M.A. Sammons, P.M. Odorizzi, S. Manne, J. Godec, O. Khan, et al., Epigenetic stability of exhausted T cells limits durability of reinvigoration by PD-1 blockade, Science 354 (6316) (2016) 1160–1165. PubMed PMID: 27789795; PubMed Central PMCID: PMCPMC5484795.

[45] A.O. Kamphorst, A. Wieland, T. Nasti, S. Yang, R. Zhang, D.L. Barber, et al., Rescue of exhausted CD8 T cells by PD-1-targeted therapies is CD28-dependent, Science 355 (6332) (2017) 1423–1427. PubMed PMID: 28280249; PubMed Central PMCID: PMCPMC5595217.

[46] Y. Shindo, K. Yoshimura, A. Kuramasu, Y. Watanabe, H. Ito, T. Kondo, et al., Combination immunotherapy with 4-1BB activation and PD-1 blockade enhances antitumor efficacy in a mouse model of subcutaneous tumor, Anticancer Res. 35 (1) (2015) 129–136. Epub 2015/01/01. PubMed PMID: 25550543.

[47] C. Chester, S. Ambulkar, H.E. Kohrt, 4-1BB agonism: adding the accelerator to cancer immunotherapy, Cancer Immunol. Immunother. : CII 65 (10) (2016) 1243–1248. PubMed PMID: 27034234; PubMed Central PMCID: PMCPMC5035667.

[48] S. Yentz, D. Smith, Indoleamine 2,3-dioxygenase (IDO) inhibition as a strategy to augment cancer immunotherapy, BioDrugs 32 (4) (2018) 311–317. PubMed PMID: 29980987.

[49] J. Galon, D. Bruni, Approaches to treat immune hot, altered and cold tumours with combination immunotherapies, Nat. Rev. Drug Discov. 18 (3) (2019) 197–218. PubMed PMID: 30610226.
[50] X. Cheng, G. Zhao, Y. Zhao, Combination immunotherapy approaches for pancreatic cancer treatment, Canadian J. Gastroenterol. Hepatol. 2018 (2018), 6240467. PubMed PMID: 29707526; PubMed Central PMCID: PMCPMC5863289.
[51] D.M. Pardoll, The blockade of immune checkpoints in cancer immunotherapy, Nat. Rev. Cancer 12 (4) (2012) 252–264. PubMed PMID: 22437870; PubMed Central PMCID: PMCPMC4856023.
[52] P.A. Ott, F.S. Hodi, H.L. Kaufman, J.M. Wigginton, J.D. Wolchok, Combination immunotherapy: a road map, Journal for immunotherapy of cancer 5 (2017) 16. PubMed PMID: 28239469; PubMed Central PMCID: PMCPMC5319100.
[53] M.E. Marmarelis, C. Aggarwal, Combination immunotherapy in non-small cell lung cancer, Curr. Oncol. Rep. 20 (7) (2018) 55. PubMed PMID: 29740718.
[54] P. Yu, J.C. Steel, M. Zhang, J.C. Morris, T.A. Waldmann, Simultaneous blockade of multiple immune system inhibitory checkpoints enhances antitumor activity mediated by interleukin-15 in a murine metastatic colon carcinoma model, Clin. Cancer Res. 16 (24) (2010) 6019–6028. PubMed PMID: 20924130; PubMed Central PMCID: PMCPMC3005104.
[55] G.P. Dunn, A.T. Bruce, H. Ikeda, L.J. Old, R.D. Schreiber, Cancer immunoediting: from immunosurveillance to tumor escape, Nat. Immunol. 3 (11) (2002) 991–998. PubMed PMID: 12407406.
[56] A. Corthay, Does the immune system naturally protect against cancer? Front. Immunol. 5 (2014) 197. PubMed PMID: 24860567; PubMed Central PMCID: PMCPMC4026755.
[57] M. Witzens-Harig, D. Hose, S. Jünger, C. Pfirschke, N. Khandelwal, L. Umansky, et al., Tumor cells in multiple myeloma patients inhibit myeloma-reactive T cells through carcinoembryonic antigen-related cell adhesion molecule-6, Blood 121 (22) (2013) 4493–4503. PubMed PMID: 23603913.
[58] B. Höchst, F.A. Schildberg, J. Böttcher, C. Metzger, S. Huss, A. Türler, et al., Liver sinusoidal endothelial cells contribute to CD8 T cell tolerance toward circulating carcinoembryonic antigen in mice, Hepatology 56 (5) (2012) 1924–1933. PubMed PMID: 22610745.
[59] C. Sautès-Fridman, F. Petitprez, J. Calderaro, W.H. Fridman, Tertiary lymphoid structures in the era of cancer immunotherapy, Nat. Rev. Cancer 19 (6) (2019) 307–325. PubMed PMID: 31092904.
[60] H. Borghaei, L. Paz-Ares, L. Horn, D.R. Spigel, M. Steins, N.E. Ready, et al., Nivolumab versus docetaxel in advanced nonsquamous non-small-cell lung cancer, N. Engl. J. Med. 373 (17) (2015) 1627–1639. Epub 2015/09/29.
[61] A.F. Chatziioannou, PET scanners dedicated to molecular imaging of small animal models, Mol. Imag. Biol. 4 (1) (2002) 47–63. PubMed PMID: 14538048.
[62] C. Kosugi, N. Saito, K. Murakami, A. Ochiai, K. Koda, M. Ono, et al., Positron emission tomography for preoperative staging in patients with locally advanced or metastatic colorectal adenocarcinoma in lymph node metastasis, Hepato-Gastroenterol. 55 (82-83) (2008) 398–402. Epub 2008/07/11. PubMed PMID: 18613374.
[63] S. Okamoto, T. Shiga, K. Yasuda, Y.M. Ito, K. Magota, K. Kasai, et al., High reproducibility of tumor hypoxia evaluated by 18F-fluoromisonidazole PET for head and neck cancer, J. Nucl. Med. 54 (2) (2013) 201–207. PubMed PMID: 23321456.
[64] D. Li, S. Cheng, S. Zou, D. Zhu, T. Zhu, P. Wang, et al., Immuno-PET imaging of (89) Zr labeled anti-PD-L1 domain antibody, Mol. Pharm. 15 (4) (2018) 1674–1681. PubMed PMID: 29502426.
[65] J. Fucikova, O. Kepp, L. Kasikova, G. Petroni, T. Yamazaki, P. Liu, et al., Detection of immunogenic cell death and its relevance for cancer therapy, Cell Death Dis. 11 (11) (2020) 1013. PubMed PMID: 33243969; PubMed Central PMCID: PMCPMC7691519.
[66] J. Marshall, Carcinoembryonic antigen-based vaccines, Semin. Oncol. 30 (8) (2003) 30–36. PubMed PMID: 12881810.
[67] A. Karube, J. Suzuki, G. Haraguchi, Y. Maejima, H. Saiki, H. Kosuge, et al., Suppression of neointimal hyperplasia after vascular injury by blocking 4-1BB/4-1BB ligand pathway, J. Med. Dent. Sci. 55 (2) (2008) 207–213. Epub 2008/06/01. PubMed PMID: 19697509.